

This discussion paper is/has been under review for the journal Biogeosciences (BG).
Please refer to the corresponding final paper in BG if available.

Global spatiotemporal distribution of soil respiration modeled using a global database

S. Hashimoto¹, N. Carvalhais^{2,3}, A. Ito^{4,5}, M. Migliavacca², K. Nishina⁶, and M. Reichstein²

¹Forestry and Forest Products Research Institute, Tsukuba, Japan

²Max Planck Institute for Biogeochemistry, Jena, Germany

³Departamento de Ciências e Engenharia do Ambiente, Universidade Nova de Lisboa, Caparica, Portugal

⁴Center for Global Environmental Research, National Institute for Environmental Studies, Tsukuba, Japan

⁵Japan Agency for Marine–Earth Science and Technology, Yokohama, Japan

⁶Center for Regional Environmental Research, National Institute for Environmental Studies, Tsukuba, Japan

Received: 24 February 2015 – Accepted: 25 February 2015 – Published: 12 March 2015

Correspondence to: S. Hashimoto (shojih@ffpri.affrc.go.jp)

Published by Copernicus Publications on behalf of the European Geosciences Union.

Title Page

Abstract

Introduction

Conclusions

References

Tables

Figures

◀

▶

◀

▶

Back

Close

Full Screen / Esc

Printer-friendly Version

Interactive Discussion



Abstract

The flux of carbon dioxide from the soil to the atmosphere (soil respiration) is one of the major fluxes in the global carbon cycle. At present, the accumulated field observation data cover a wide range of geographical locations and climate conditions. However, there are still large uncertainties in the magnitude and spatiotemporal variation of global soil respiration. Using a global soil respiration dataset, we developed a climate-driven model of soil respiration by modifying and updating Raich's model, and the global spatiotemporal distribution of soil respiration was examined using this model. The model was applied at a spatial resolution of 0.5° and a monthly time step. Soil respiration was divided into the heterotrophic and autotrophic components of respiration using an empirical model. The estimated mean annual global soil respiration was 91 PgCyr^{-1} (between 1965 and 2012; Monte Carlo 95% confidence interval: $87\text{--}95 \text{ PgCyr}^{-1}$) and increased at the rate of 0.09 PgCyr^{-2} . The contribution of soil respiration from boreal regions to the total increase in global soil respiration was on the same order of magnitude as that of tropical and temperate regions, despite a lower absolute magnitude of soil respiration in boreal regions. The estimated annual global heterotrophic respiration and global autotrophic respiration were 51 and 40 PgCyr^{-1} , respectively. The global soil respiration responded to the increase in air temperature at the rate of $3.3 \text{ PgCyr}^{-1} \text{ }^\circ\text{C}^{-1}$, and $Q_{10} = 1.4$. Our study scaled up observed soil respiration values from field measurements to estimate global soil respiration and provide a data-oriented estimate of global soil respiration. Our results, including the modeled spatiotemporal distribution of global soil respiration, are based on a semi-empirical model parameterized with over one thousand data points. We expect that these spatiotemporal estimates will provide a benchmark for future studies and also help to constrain process-oriented models.

Global spatiotemporal distribution of soil respiration

S. Hashimoto et al.

Title Page

Abstract

Introduction

Conclusions

References

Tables

Figures



Back

Close

Full Screen / Esc

Printer-friendly Version

Interactive Discussion



1 Introduction

The carbon balance of terrestrial ecosystems is the result of the balance between carbon uptake by plants and carbon loss by plant and soil respiration (Beer et al., 2010; Luyssaert et al., 2007; Malhi et al., 1999; Le Quéré et al., 2009, 2014; Trumbore, 2006). The value of the balance, i.e., whether terrestrial ecosystems act as sinks or sources of carbon, has been a subject of considerable interest for studies of climate change. Accurate evaluations of each sink/source component and their response to environmental factors are thus essential for understanding future changes in the terrestrial carbon balance.

The carbon dioxide (CO_2) flux from the soil to the atmosphere (called soil respiration, R_S) is one of the major fluxes in the global carbon cycle (Schlesinger and Andrews, 2000). R_S primarily consists of heterotrophic respiration (soil organic matter decomposition) and autotrophic respiration (root respiration) (Bond-Lamberty et al., 2004; Hanson et al., 2000). R_S is the main contributor to the total ecosystem respiration (Malhi et al., 1999); hence, R_S plays a role in determining the carbon balance of terrestrial ecosystems. R_S is sensitive to environmental factors (e.g., temperature and precipitation) (Davidson et al., 1998; Hashimoto et al., 2011b; Raich and Schlesinger, 1992; Raich et al., 2002; Schlesinger and Andrews, 2000), and future climate change is expected to increase the rate of R_S at the global scale (Bond-Lamberty and Thomson, 2010b; Hashimoto et al., 2011a; Raich et al., 2002). Even a small change in the global R_S rate will have a strong impact on the terrestrial carbon cycle and may accelerate the increase in the atmospheric CO_2 concentration (IPCC, 2001, 2007).

Observations of R_S have a long history; in particular, the amount of collected field data increased rapidly in the 1990s, and there are now thousands of records of observed data (Bond-Lamberty and Thomson, 2010a; Chen et al., 2014). Recently, a global dataset of observed R_S was established by collecting data from available studies published in the peer-reviewed scientific literature (Bond-Lamberty and

BGD

12, 4331–4364, 2015

Global spatiotemporal distribution of soil respiration

S. Hashimoto et al.

Title Page

Abstract

Introduction

Conclusions

References

Tables

Figures

◀

▶

◀

▶

Back

Close

Full Screen / Esc

Printer-friendly Version

Interactive Discussion



Thomson, 2010a). The use of the accumulated data for field observations will improve the estimation of global R_S .

The number of global estimates of R_S is, however, quite limited compared to the estimates of other terrestrial carbon fluxes (e.g., gross and net primary production (GPP and NPP, respectively)), or other greenhouse gas fluxes (e.g., methane and nitrous oxide). For instance, based on a literature survey (Ito, 2011), there are at least 251 estimates of global NPP. For R_S , to the best of our knowledge, there are only six global estimates, ranging from 68 to 98 PgCyr⁻¹ and, thus, characterized by a large uncertainty (Hashimoto, 2012). Another example that indicates the large uncertainty in estimating R_S are the large variations in estimates of soil carbon stocks and heterotrophic respiration simulated by the state-of-the-art Earth system models of the Coupled Model Intercomparison Project Phase 5 (CMIP5; <http://cmip-pcmdi.llnl.gov/cmip5/>) (Exbrayat et al., 2014; Todd-Brown et al., 2013), which is a model intercomparison project that provides scientific knowledge to the Intergovernmental Panel on Climate Change (Taylor et al., 2012). These facts suggest that further efforts should attempt to constrain the estimate of global R_S by employing a model-data integration approach and field measurements.

The purpose of this study was to provide a new global estimate of the spatiotemporal distribution of R_S based on the available observational datasets. Using a global R_S dataset (Bond-Lamberty and Thomson, 2010a), we developed a semi-empirical climate-driven model for R_S . The temperature and precipitation functions of Raich's model were refined, and the parameters of the model were newly determined using over one thousand data points. We explored the spatiotemporal distribution of R_S and examined the temperature sensitivity of R_S . We further divided the estimated global R_S into the heterotrophic and autotrophic components of R_S using an empirical relationship between R_S and heterotrophic respiration and examined the distribution of each type of respiration.

**Global
spatiotemporal
distribution of soil
respiration**

S. Hashimoto et al.

Title Page

Abstract

Introduction

Conclusions

References

Tables

Figures



Back

Close

Full Screen / Esc

Printer-friendly Version

Interactive Discussion



2 Materials and methods

2.1 Models

We developed a climate-driven model by updating Raich's model (Raich and Potter, 1995; Raich et al., 2002). The original model, Eq. (1), simulates the R_S as a function of temperature and water (precipitation), and its sensitivities are parameterized using three constants (F , K , and Q). The model is applied at a monthly time step and requires the monthly mean air temperature (T , °C) and monthly precipitation (P , cm).

$$\text{mo}R_S = F \cdot e^{Q \cdot T} \cdot \frac{P}{K + P}, \quad (1)$$

where, $\text{mo}R_S$ is the mean monthly R_S ($\text{gCm}^{-2} \text{d}^{-1}$), and F ($\text{gCm}^{-2} \text{d}^{-1}$), Q ($^{\circ}\text{C}^{-1}$), and K (cm mo^{-1}) are the parameters. The advantage of this model is its simplicity. Although there are numerous factors that affect R_S (Chen et al., 2014), it is often recognized that temperature and precipitation are the two best predictors to represent the spatiotemporal variability of R_S (Bond-Lamberty and Thomson, 2010b). In this study, the temperature and water functions of the original model were modified as follows:

$$\text{mo}R_S = F \cdot e^{(aT - bT^2)} \cdot \frac{\alpha P + (1 - \alpha)P_{m-1}}{K + \alpha P + (1 - \alpha)P_{m-1}} \quad (2)$$

where, F ($\text{gCm}^{-2} \text{d}^{-1}$) and K (cm mo^{-1}) are the parameters; a ($^{\circ}\text{C}^{-1}$) and b ($^{\circ}\text{C}^{-2}$) are the parameters for the temperature function; and α is the parameter for the precipitation function; P_{m-1} (cm) is the precipitation of the previous month.

First, we introduced a more flexible temperature function that has been reported to behave better than the simple exponential temperature function (Tuomi et al., 2008). This function peaks at $T = a(2b)^{-1}$, and the function can take either a convex shape or a simple exponential-like shape depending on the parameters a and b . The simple

exponential temperature function has been widely applied to the modeling of the temperature sensitivity of R_S , but a limitation is often pointed out in that the Q_{10} value (the factor by which the respiration rate increases for a temperature interval of 10°C) of the exponential function does not change across temperature, while analyses of observed temperature sensitivities of R_S suggest that the Q_{10} value decreases with an increase in temperature (Kirschbaum, 1995; Tuomi et al., 2008) (but see Mahecha et al., 2010). The Q_{10} value of the new temperature function can change across temperature ranges.

Second, we adopted the weighted average of the precipitation of both the current month and the previous month instead of only using the precipitation of the current month. One of the limitations of the precipitation function of the original model was the so-called “zero-precipitation-zero-respiration” problem (Reichstein et al., 2003). In the original precipitation function, R_S becomes zero when precipitation of the present month is zero; however, although zero precipitation occurs at times, even in temperate regions, R_S can be maintained. However, this assumption of R_S is reasonable when we focus on a global-scale evaluation and distinguish between very dry regions, such as deserts, and other regions. Including a soil water sub model to simulate the soil water conditions would be one solution, but we used a weighted average of precipitation here to avoid model complexity.

2.2 Dataset

The R_S data used in this study were obtained from the SRDB database (Bond-Lamberty and Thomson, 2010a) (version 3). The database covers a wide range of geographical and climatic spaces (Fig. S1 in the Supplement), although the availability of is limited for certain regions (i.e., with low temperature, and with high temperature and low precipitation). For the purpose of modeling, the data from non-experimentally manipulated, non-agricultural ecosystems that had been measured using an infrared gas analyzer or gas chromatograph were extracted. The data with quality check flags, except for Q01, Q02, and Q03, were excluded. We further extracted the data with

Global spatiotemporal distribution of soil respiration

S. Hashimoto et al.

Title Page

Abstract

Introduction

Conclusions

References

Tables

Figures



Back

Close

Full Screen / Esc

Printer-friendly Version

Interactive Discussion



the location information (latitude and longitude) to support their combination with the monthly climate data from the global climate dataset. The air temperature and precipitation were derived from the CRU3.21 climate data (University of East Anglia Climatic Research Unit (CRU), Jones and Harris, 2013). The number of data points used for model parameterization was 1638.

We examined other models that included leaf area index (LAI) and GPP for the parameterization of F in Eq. (1) (Mahecha et al., 2010; Migliavacca et al., 2011; Reichstein et al., 2003) (Table S1 in the Supplement). The model with LAI and GPP was characterized by a higher R^2 value than the simple climate-driven model (Table S1), which supports the hypothesis that vegetation substantially influences the variation in R_S (Migliavacca et al., 2011; Reichstein et al., 2003; Wang et al., 2010). However, the number of data points in the database with LAI and GPP were limited, and including LAI and GPP resulted in losses of over 70 and 90 % of the data points, respectively (Table S1) (e.g., Bond-Lamberty and Thomson, 2010b). For the purpose of providing global estimates based on the accumulated observed data, we placed a higher value on relatively larger data points that cover wider geographical and climatic spaces rather than building additional mechanistic models. Hence, the above-described climate-driven model was adopted for the estimation of global R_S in this study. Similar to previous studies, the impact of land use change was not included in this study.

2.3 Parameterization

We used a Bayesian calibration scheme to determine the best parameter sets and their uncertainty (Bates and Campbell, 2001; Hashimoto et al., 2011b; Van Oijen et al., 2005; Ricciuto et al., 2008; Zobitz et al., 2008). We assumed a uniform distribution for the a priori distribution of every parameter (F, a, b, K, α) and assumed a Gaussian model-data error (SD: σ). To generate the a posteriori distribution, we performed a Markov Chain Monte Carlo simulation (MCMC) based on the Metropolis–Hastings (M–H) algorithm; the log-likelihood was used in practice. We conducted 100 000 iterations of sampling and discarded the first 20 000 iterations as the burn-

Global spatiotemporal distribution of soil respiration

S. Hashimoto et al.

Title Page

Abstract

Introduction

Conclusions

References

Tables

Figures



Back

Close

Full Screen / Esc

Printer-friendly Version

Interactive Discussion



in period. The maximum a posteriori estimates (MAP) were designated as the best-fit parameters. Geweke's Z score was calculated for convergence diagnostics (Geweke, 1992); a Geweke's Z score range of ± 1.96 indicates convergence (significance level of 5%).

2.4 Global application

The R_S was evaluated at a spatial resolution of 0.5° and a monthly time resolution. The air temperature and precipitation were derived from the CRU 3.21 climate data (University of East Anglia Climatic Research Unit (CRU), Jones and Harris, 2013). The global land-use data in SYNMAP (Jung et al., 2006) were converted to 0.5° for use in this study. We calculated the R_S for the period from 1965 to 2012. A Monte Carlo simulation was applied to evaluate the uncertainty of the estimates; the model was run 1000 times using the parameter uncertainties derived from the Bayesian calibration.

2.5 Partitioning the total R_S into the heterotrophic (R_H) and autotrophic (R_A) respiration components

The estimated annual R_S was divided into heterotrophic respiration (R_H) and autotrophic respiration (R_A) using an empirical relationship derived by a meta-analysis (Bond-Lamberty et al., 2004). From that meta-analysis, a global relationship between the heterotrophic and autotrophic components of R_S was established from the analysis of published data. We adopted this relationship:

$$\ln(\text{an}R_H) = 1.22 + 0.73 \ln(\text{an}R_S). \quad (3)$$

The annual R_H ($\text{an}R_H$) was estimated by substituting the calculated annual R_S ($\text{an}R_S$) into the above-described relationship. The annual R_A was then calculated by subtracting the annual R_H from the annual R_S .

BGD

12, 4331–4364, 2015

Global spatiotemporal distribution of soil respiration

S. Hashimoto et al.

Title Page

Abstract

Introduction

Conclusions

References

Tables

Figures

◀

▶

◀

▶

Back

Close

Full Screen / Esc

Printer-friendly Version

Interactive Discussion



2.6 Comparison with Earth system models

The estimated R_H was compared with the estimates from Earth system models provided by CMIP5. We calculated global R_H using 20 Earth system models of the CMIP5 (Table S2) and compared the results with our estimate.

2.7 Statistical analysis

We defined tropical, temperate, and boreal regions based on the annual temperature ($T < 2^\circ\text{C}$, $2 \leq T \leq 17^\circ\text{C}$, $17^\circ\text{C} < T$) after a previous study (Bond-Lamberty and Thomson, 2010b). Statistical analyses were conducted using R versions 3.0.2 and 3.1.0 (R Core team, 2013). The Mann–Kendall trend test was applied to test for the significance of trends (R package, Kendall version 2.2).

3 Results

Table 1 lists the a priori and a posteriori distributions of the parameters, and the estimated best parameters with their uncertainties and statistics. The temperature function and precipitation function developed in this study are depicted in Fig. 1, and the two original functions are also plotted. Regarding the temperature function, the three lines were approximately overlapping under 10°C , but the differences among the three lines increased with an increase in temperature. The temperature sensitivity of the newly estimated function was attenuated at high temperatures compared to the simple exponential functions applied in the original temperature functions, for which the temperature sensitivity steadily increased. Depending upon the parameterization, the newly introduced function can either peak at a certain temperature or behave as a simple exponential function. Our parameterization did not result in a peak in this temperature range, but the temperature sensitivity decreased as the temperature increased. The newly estimated precipitation function was similar to that of the previous study (Raich and Potter, 1995); note that the precipitation used in this study is the

weighted average of the precipitation of the current month and the previous month. The best value for the weighting factor α was 0.98, but α was characterized by a large uncertainty (0.03–0.99, 95 % confidence interval).

The estimated mean annual global R_S was 91 PgCyr⁻¹ (1965–2012; Monte Carlo 95 % confidence interval: 87–95 PgCyr⁻¹), and the spatial distribution of R_S is depicted in Fig. 2. The estimated R_S was high in tropical regions and low in boreal regions, following a temperature-oriented gradient from near the equator to higher latitudes, but the estimated values were low in dry regions as well (Fig. 2a and b). Latitudinally, the regions between 30° S and 30° N contributed the most to global R_S , but the contribution of the region between 30 and 60° N was also large (Fig. 2c). The contributions of the tropical, temperate, and boreal regions were 64, 24, and 12 %, respectively, of global R_S . The monthly global R_S was lowest in February (5.7 PgC mo⁻¹) and greatest in July (9.4 PgC mo⁻¹) (Figs. S2 and S3). The mean annual grid-cell R_S was characterized by a broad distribution, ranging from 0 to greater than 1500 gC m⁻² yr⁻¹ (Fig. S4).

The estimated R_S followed an increasing trend over time, with fluctuations, and the rate of the estimated increase was 0.09 PgCyr⁻² ($P < 0.0001$) between 1965 and 2012 and 0.14 PgCyr⁻² ($P = 0.0015$) between 1990 and 2012 (Fig. 3, Table S3 i). The lowest value of R_S (88 PgCyr⁻¹) occurred in both 1965 and 1970, and the highest value (95 PgCyr⁻¹) occurred in 2010. The higher and lower values were mainly coincident with El Niño Southern Oscillation events. The trends were examined for the tropical, temperate, and boreal regions: the annual variation was largest in tropical regions and was lowest in boreal regions (Figs. 4 and S5). In tropical regions, large fluctuations in R_S occurred during the 1970s. In all regions, the R_S followed an increasing trend with time. The rates of increase in R_S for the tropical, temperate, and boreal regions were 0.048 ($P < 0.0001$), 0.025 ($P < 0.0001$), and 0.021 ($P < 0.0001$) PgCyr⁻², respectively; hence, the highest rates of increase occurred in the tropical regions. The proportional increases in the R_S of the tropical, temperate, and boreal regions were 0.08, 0.11, and 0.19 %, respectively; thus, the proportional increase was greatest for the boreal regions. The difference between the earlier and later period of

Global spatiotemporal distribution of soil respiration

S. Hashimoto et al.

[Title Page](#)[Abstract](#)[Introduction](#)[Conclusions](#)[References](#)[Tables](#)[Figures](#)[⏪](#)[⏩](#)[◀](#)[▶](#)[Back](#)[Close](#)[Full Screen / Esc](#)[Printer-friendly Version](#)[Interactive Discussion](#)

the simulation is shown by latitude in Fig. 2d. The R_S increased at nearly all latitudes. There were large increases in R_S between 0 and 30° N and between 30 and 70° N.

The relationship between the annual mean global temperature and the global R_S is characterized by a slope of 3.3 PgCyr⁻¹°C⁻¹ ($P < 0.0001$) (Fig. 5) and a Q_{10} value of 1.4. Figure 6 presents the distribution of the Q_{10} values at the grid scale, which was calculated using the temperature function estimated in this study and the mean temperature of each grid. The Q_{10} values varied between 1 and 2 and were lower in the regions near the equator and higher in the regions at high latitudes with colder climates.

The estimated global R_H and R_A were 51 and 40 PgCyr⁻¹, respectively. The spatial distributions of R_H and R_A are depicted in Fig. 7. Both the R_H and the R_A were high in tropical regions and low in cold and/or dry regions. The R_H and R_A were nearly equivalent to each other, but in the regions of high R_S , R_H was greater than R_A ; and in the regions with low R_S , R_A was greater than R_H . The distribution of the $R_A : R_S$ ratio indicates that, in tropical and temperate regions, the R_A component contributes approximately 40–50% of R_S , while R_A accounted for less than 30% of R_S in cold and/or dry regions (Fig. 8).

Figure 9 compares the R_H estimated by our model to those estimated using other Earth system models. The value of R_H estimated by the Earth system models varied from 40 to greater than 77 PgCyr⁻¹. The mean of the results from the Earth system models (54 PgCyr⁻¹, 1965–2004) was similar to our estimate. The latitudinal distributions of R_H differed among the Earth system models (Fig. 10). In particular, the differences among models were large between 30° S and 10° N and from 40 to 70° N. The distribution of the R_H estimated using this model was primarily in accordance with the mean of Earth system models; however, a large difference was noted between 10° S and 10° N.

BGD

12, 4331–4364, 2015

Global spatiotemporal distribution of soil respiration

S. Hashimoto et al.

Title Page

Abstract

Introduction

Conclusions

References

Tables

Figures

◀

▶

◀

▶

Back

Close

Full Screen / Esc

Printer-friendly Version

Interactive Discussion



4 Discussion

4.1 Spatiotemporal distribution of R_S

Overall, the estimated R_S was high in tropical regions and low in cold and/or dry regions. The model parameters derived from the parameterization (Table 1 and Fig. 1) indicate that the R_S increases under conditions of high temperature and high precipitation. Our modeling suggests that the spatial distribution of R_S at global scale is controlled by both precipitation and temperature (Figs. 2a and S6). These patterns basically agree with those reported in previous studies (Bond-Lamberty and Thomson, 2010b; Chen et al., 2010; Hashimoto, 2012; Raich et al., 2002). However, the estimated total global R_S of this study (91 Pg C yr^{-1}) differs from the results of the previous studies. Previous estimates can be roughly divided into two categories, the highest estimate of 98 Pg C yr^{-1} (Bond-Lamberty and Thomson, 2010b) and the other estimates (76 Pg C yr^{-1} , on average, $N = 5$) (Hashimoto, 2012; Raich and Potter, 1995; Raich and Schlesinger, 1992; Raich et al., 2002; Schlesinger, 1977) (Table S4). Our estimate is based on the same dataset as that analyzed for the highest estimate (Bond-Lamberty and Thomson, 2010b), but the new estimate of this study was 7% lower than that estimate. We speculate that one of the reasons for this difference might be the differences in model structure. A non-linear model was used in this study, while linear models were employed in the previous study. In particular, we assumed that R_S is sensibly reduced when the sum of precipitation of the current month and previous month is zero. The R_S was very low in dry regions (e.g., deserts in Africa and Mongolia) (Fig. 2). The numbers of observations are quite limited for very dry regions and deserts; for this reason, although we considered that it is reasonable to assume approximately zero-respiration in these regions, we should consider the potentially high uncertainty in these estimates. However, the new estimate was higher than other previous estimates (i.e., all of the estimates other than Bond-Lamberty and Thomson, 2010b). In particular, the new estimate was higher than that of Raich et al. (2002) despite using nearly the

same model structure. We attribute this difference to the differences in the datasets analyzed for parameterization (Table S1 and Fig. S7).

The global R_S followed an increasing trend, and the rate of the increase was comparable to that estimated by a previous study (Bond-Lamberty and Thomson, 2010b). Our model did not include a detailed carbon cycle for the evaluated ecosystems; hence, it is not possible to argue that this increasing trend indicates a net loss of carbon from the soil to the atmosphere (Gottschalk et al., 2012; Smith and Fang, 2010). However, our analysis provides additional data to support an increasing trend for global R_S , even though a new model was applied for this study, and supports the assumption that the soil carbon flux from soil to the atmosphere is increasing in response to climate change.

4.2 Heterotrophic and autotrophic respirations

Although the number of reports of R_H is limited, our estimate of R_H is comparable to those of previous studies (IPCC, 2001; Potter and Klooster, 1997). In addition, the mean value of R_H estimated using the Earth system models is comparable to our estimate (Fig. 9). This agreement might imply that the carbon cycles in the Earth system models are, to an extent, well constrained by the carbon influx terms (GPP and NPP), and there are, in comparison to R_H , numerous global estimates for GPP and NPP. However, when we look at the results from each Earth system model, the differences among estimates are distinct in terms of the magnitude and spatial distribution. Because the air temperature simulated by the models in CMIP5 is well correlated with temperature of a CRU (Todd-Brown et al., 2013), the variation in R_H might be attributable to the differences in the description of the terrestrial carbon cycle in each model. R_H is a major carbon flux in an ecosystem carbon cycle; therefore, the large variation in R_H indicates that there are large uncertainties in the overall flows of carbon in ecosystems (e.g., photosynthesis and respiration) associated with the Earth system model. In fact, there are large variations among estimates of soil carbon stocks and soil carbon responses to

BGD

12, 4331–4364, 2015

Global spatiotemporal distribution of soil respiration

S. Hashimoto et al.

Title Page

Abstract

Introduction

Conclusions

References

Tables

Figures

⏪

⏩

◀

▶

Back

Close

Full Screen / Esc

Printer-friendly Version

Interactive Discussion



climate change generated using Earth system models (Carvalho et al., 2014; Nishina et al., 2014; Todd-Brown et al., 2013).

The estimated global-scale contribution of R_A (root respiration) to total R_S was 44%. At the grid scale, there was considerable variation in the $R_A : R_S$ ratio, which is in agreement with the reports based on compilations of previous laboratory and field studies (Hanson et al., 2000). However, although there are observational reports of $R_A : R_S$ ratio greater than 0.5, such high $R_A : R_S$ ratios were not observed in our modeling study because of the relationship between R_S and R_H applied in this study. Another reason might be that the compilation studies included data observed under various vegetation/soil conditions and seasons, while our study provides a spatiotemporal average. For example, the $R_A : R_S$ ratio will be high in densely planted vegetation.

4.3 Contributions of tropical, temperate, and boreal regions

Our study, similar to previous studies, revealed that tropical regions contribute the largest proportion of global R_S (Bond-Lamberty and Thomson, 2010b; Hashimoto, 2012; Raich et al., 2002). This finding is not surprising because R_S responds to temperature exponentially and also because there are large amounts of litter input to soil in tropical regions. However, strikingly, the contribution of R_S from boreal regions to the rate of increase in R_S at the global scale for the study period was on the same order of magnitude with that of the contributions from tropical and temperate regions despite the lower contribution of R_S from boreal regions to the total global R_S in terms of absolute magnitude. This relatively large contribution is attributed to the temperature sensitivity of R_S (quasi-linear response) and the magnitude of the temperature increase in boreal regions, which was greater than the increase for tropical regions. At present, tropical regions are the most influential regions in terms of global R_S (e.g., 64% of the global R_S based on our results). As suggested in previous studies, the importance of boreal regions in global carbon cycle is increasing and will continue to increase

BGD

12, 4331–4364, 2015

Global spatiotemporal distribution of soil respiration

S. Hashimoto et al.

Title Page

Abstract

Introduction

Conclusions

References

Tables

Figures

⏪

⏩

◀

▶

Back

Close

Full Screen / Esc

Printer-friendly Version

Interactive Discussion



analyses conducted at multiple spatiotemporal scales (e.g., Kirschbaum, 2010; Subke and Bahn, 2010). When process-oriented ecosystem models are applied at the field or grid scale and then scaled up to the global scale, comparisons of the global scale temperature sensitivity of such scaling efforts with the results of our study may be useful for examining whether R_S has been properly scaled.

4.5 Conclusions and future work

In this study, we estimated the spatiotemporal variation of global R_S using a global soil database, SRDB, and a semi-empirical model. The study scaled up the observed field-scale R_S values to a global-scale R_S to provide a data-oriented estimate of global R_S . The estimated mean annual global R_S was 91 PgCyr^{-1} (1965–2012; Monte Carlo 95 % confidence interval: $87\text{--}95 \text{ PgCyr}^{-1}$), which differs from those of previous studies. Our model does not include detailed processes for ecosystem carbon cycles, imparting both limitations and advantages to this study. For example, plant photosynthesis, belowground carbon allocation, land-use changes, and nitrogen transformations can affect R_S , and in particular, these processes play important roles in long-term simulations of terrestrial carbon cycles. In regards to boreal regions, the impact of permafrost melting was not considered in this study, which is an important process in northern regions. However, simple semi-empirical models are good at assimilating accumulated observed field data and providing data-oriented estimations. The relationship between R_H and R_S is derived from data observations for forest ecosystems, which could affect our estimate of R_H . The resolution of our analysis is coarse compared to the scale of the field observations.

Our study has demonstrated that the accumulated data for R_S can be used to develop simple, data-oriented models, but in the future, datasets that include other related processes/properties (e.g., LAI, and GPP) will be necessary to generate relatively more sophisticated, simple models and to further constrain process-oriented models. Nevertheless, our approach, the use of a simple model for the analysis of accumulated

BGD

12, 4331–4364, 2015

Global spatiotemporal distribution of soil respiration

S. Hashimoto et al.

Title Page

Abstract

Introduction

Conclusions

References

Tables

Figures

◀

▶

◀

▶

Back

Close

Full Screen / Esc

Printer-friendly Version

Interactive Discussion



data resources, provides data-oriented estimates and can be used to bridge a gap between process-oriented modeling and observed datasets. We expect that our data-oriented, spatiotemporal estimates will serve as benchmarks and also help to constrain process-oriented models and Earth system models.

5 **The Supplement related to this article is available online at
doi:10.5194/bgd-12-4331-2015-supplement.**

Acknowledgements. This study was supported by JSPS KAKENHI 24510025. S. Hashimoto thanks B. Bond-Lamberty and A. Thomson for the use of their global dataset of soil respiration and also thanks the Forestry and Forest Products Research Institute, the Max-Plank-Institute
10 for Biogeochemistry Jena, and the National Institute for Environmental Studies.

References

- Bates, B. C. and Campbell, E. P.: A Markov chain Monte Carlo scheme for parameter estimation and inference, *Water Resour. Res.*, 37, 937–947, 2001.
- Batjes, N. H.: Total carbon and nitrogen in the soils of the world, *Eur. J. Soil Sci.*, 47, 151–163,
15 doi:10.1111/j.1365-2389.1996.tb01386.x, 1996.
- Beer, C., Reichstein, M., Tomelleri, E., Ciais, P., Jung, M., Carvalhais, N., Rödenbeck, C., Arain, M. A., Baldocchi, D., Bonan, G. B., Bondeau, A., Cescatti, A., Lasslop, G., Lindroth, A., Lomas, M., Luyssaert, S., Margolis, H., Oleson, K. W., Rouspard, O., Veenendaal, E., Viovy, N., Williams, C., Woodward, F. I., and Papale, D.: Terrestrial gross carbon dioxide uptake: global distribution and covariation with climate, *Science*, 329, 834–838, doi:10.1126/science.1184984, 2010.
- Bond-Lamberty, B. and Thomson, A.: A global database of soil respiration data, *Biogeosciences*, 7, 1915–1926, doi:10.5194/bg-7-1915-2010, 2010a.
- Bond-Lamberty, B. and Thomson, A.: Temperature-associated increases in the global soil
20 respiration record, *Nature*, 464, 579–582, doi:10.1038/nature08930, 2010b.

BGD

12, 4331–4364, 2015

Global spatiotemporal distribution of soil respiration

S. Hashimoto et al.

Title Page

Abstract

Introduction

Conclusions

References

Tables

Figures

◀

▶

◀

▶

Back

Close

Full Screen / Esc

Printer-friendly Version

Interactive Discussion



Global spatiotemporal distribution of soil respiration

S. Hashimoto et al.

Title Page

Abstract

Introduction

Conclusions

References

Tables

Figures



Back

Close

Full Screen / Esc

Printer-friendly Version

Interactive Discussion



- Bond-Lamberty, B., Wang, C., and Gower, S. T.: A global relationship between the heterotrophic and autotrophic components of soil respiration?, *Glob. Change Biol.*, 10, 1756–1766, 2004.
- Carvalho, N., Forkel, M., Khomik, M., Bellarby, J., Jung, M., Migliavacca, M., Mu, M., Saatchi, S., Santoro, M., Thurner, M., Weber, U., Ahrens, B., Beer, C., Cescatti, A., Randerson, J. T., and Reichstein, M.: Global covariation of carbon turnover times with climate in terrestrial ecosystems, *Nature*, 514, 213–217, doi:10.1038/nature13731, 2014.
- Chen, S., Huang, Y., Zou, J., Shen, Q., Hu, Z., Qin, Y., Chen, H., and Pan, G.: Modeling interannual variability of global soil respiration from climate and soil properties, *Agr. Forest Meteorol.*, 150, 590–605, doi:10.1016/j.agrformet.2010.02.004, 2010.
- Chen, S., Zou, J., Hu, Z., Chen, H., and Lu, Y.: Global annual soil respiration in relation to climate, soil properties and vegetation characteristics: summary of available data, *Agr. Forest Meteorol.*, 198–199, 335–346, doi:10.1016/j.agrformet.2014.08.020, 2014.
- Davidson, E. A., Belk, E., and Boone, R. D.: Soil water content and temperature as independent or confounded factors controlling soil respiration in a temperate mixed hardwood forest, *Glob. Change Biol.*, 4, 217–227, 1998.
- Dixon, R. K., Solomon, A. M., Brown, S., Houghton, R. A., Trexler, M. C., and Wisniewski, J.: Carbon pools and flux of global forest ecosystems, *Science*, 263, 185–190, doi:10.1126/science.263.5144.185, 1994.
- Eswaran, H., Van Den Berg, E., and Reich, P.: Organic carbon in soils of the world, *Soil Sci. Soc. Am. J.*, 57, 192–194, 1993.
- Exbrayat, J.-F., Pitman, A. J., and Abramowitz, G.: Response of microbial decomposition to spin-up explains CMIP5 soil carbon range until 2100, *Geosci. Model Dev.*, 7, 2683–2692, doi:10.5194/gmd-7-2683-2014, 2014.
- Geweke, J.: Evaluating the accuracy of sampling-based approaches to the calculation of posterior moments, in: *Bayesian Statistics*, vol. 4, edited by: Bernardo, J. M., Berger, J. O., Dawid, A. P., and Smith, A. F., Oxford University Press, Oxford, 169–193, 1992.
- Gottschalk, P., Smith, J.U., Wattenbach, M., Bellarby, J., Stehfest, E., Arnell, N., Osborn, T. J., Jones, C., and Smith, P.: How will organic carbon stocks in mineral soils evolve under future climate? Global projections using RothC for a range of climate change scenarios, *Biogeosciences*, 9, 3151–3171, doi:10.5194/bg-9-3151-2012, 2012.
- Hanson, P. J., Edwards, N. T., Garten, C. T., and Andrews, J. A.: Separating root and soil microbial contributions to soil respiration: a review of methods and observations, *Biogeochemistry*, 48, 115–146, 2000.

Global spatiotemporal distribution of soil respiration

S. Hashimoto et al.

Title Page

Abstract

Introduction

Conclusions

References

Tables

Figures



Back

Close

Full Screen / Esc

Printer-friendly Version

Interactive Discussion



- Hashimoto, S.: A new estimation of global soil greenhouse gas fluxes using a simple data-oriented model, *PLoS One*, 7, e41962, doi:10.1371/journal.pone.0041962, 2012.
- Hashimoto, S., Morishita, T., Sakata, T., and Ishizuka, S.: Increasing trends of soil greenhouse gas fluxes in Japanese forests from 1980 to 2009, *Sci. Rep.-UK*, 1, 116, doi:10.1038/srep00116, 2011a.
- Hashimoto, S., Morishita, T., Sakata, T., Ishizuka, S., Kaneko, S., and Takahashi, M.: Simple models for soil CO₂, CH₄, and N₂O fluxes calibrated using a Bayesian approach and multi-site data, *Ecol. Model.*, 222, 1283–1292, doi:10.1016/j.ecolmodel.2011.01.013, 2011b.
- IPCC: Climate Change 2001: the Scientific Basis, edited by: Houghton, J. T., Ding, Y., Griggs, D. J., Noguer, M., van der Linden, P. J., Dai, X., Maskell, K., and Johnson, C. A., Cambridge University Press, Cambridge, 2001.
- IPCC: Climate Change 2007: the Physical Science Basis, edited by: Solomon, S., Qin, D., Manning, M., Marquis, M., Averyt, K., Tignor, M. M. B., Miller Jr., H. L., and Chen, Z., Cambridge University Press, Cambridge, 2007.
- Ise, T. and Moorcroft, P. R.: The global-scale temperature and moisture dependencies of soil organic carbon decomposition: an analysis using a mechanistic decomposition model, *Biogeochemistry*, 80, 217–231, doi:10.1007/s10533-006-9019-5, 2006.
- Ito, A.: A historical meta-analysis of global terrestrial net primary productivity: are estimates converging?, *Glob. Change Biol.*, 17, 3161–3175, doi:10.1111/j.1365-2486.2011.02450.x, 2011.
- Jones, C. and Cox, P. M.: Constraints on the temperature sensitivity of global soil respiration from the observed interannual variability in atmospheric CO₂, *Atmos. Sci. Lett.*, 2, 166–172, doi:10.1006/asle.2001.0041, 2001.
- Jung, M., Henkel, K., Herold, M., and Churkina, G.: Exploiting synergies of global land cover products for carbon cycle modeling, *Remote Sens. Environ.*, 101, 534–553, doi:10.1016/j.rse.2006.01.020, 2006.
- Kaminski, T., Knorr, W., Rayner, P. J., and Heimann, M.: Assimilating atmospheric data into a terrestrial biosphere model: a case study of the seasonal cycle, *Global Biogeochem. Cy.*, 16, 1066, doi:10.1029/2001GB001463, 2002.
- Kirschbaum, M. U. F.: The temperature dependence of soil organic matter decomposition, and the effect of global warming on soil organic C storage, *Soil Biol. Biochem.*, 27, 753–760, doi:10.1016/0038-0717(94)00242-S, 1995.

Kirschbaum, M. U. F.: The temperature dependence of organic matter decomposition: seasonal temperature variations turn a sharp short-term temperature response into a more moderate annually averaged response, *Glob. Change Biol.*, 16, 2117–2129, doi:10.1111/j.1365-2486.2009.02093.x, 2010.

5 Luysaert, S., Inglima, I., Jung, M., Richardson, A. D., Reichstein, M., Papale, D., Piao, S. L., Schulze, E.-D., Wingate, L., Matteucci, G., Aragao, L., Aubinet, M., Beer, C., Bernhofer, C., Black, K. G., Bonal, D., Bonnefond, J.-M., Chambers, J., Ciais, P., Cook, B., Davis, K. J., Dolman, A. J., Gielen, B., Goulden, M., Grace, J., Granier, A., Grelle, A., Griffis, T., Grünwald, T., Guidolotti, G., Hanson, P. J., Harding, R., Hollinger, D. Y., Hutyra, L. R.,
10 Kolari, P., Kruijt, B., Kutsch, W., Lagergren, F., Laurila, T., Law, B. E., Le Maire, G., Lindroth, A., Loustau, D., Malhi, Y., Mateus, J., Migliavacca, M., Misson, L., Montagnani, L., Moncrieff, J., Moors, E., Munger, J. W., Nikinmaa, E., Ollinger, S. V., Pita, G., Rebmann, C., Rouspard, O., Saigusa, N., Sanz, M. J., Seufert, G., Sierra, C., Smith, M.-L., Tang, J., Valentini, R., Vesala, T., and Janssens, I. A.: CO₂ balance of boreal, temperate, and
15 tropical forests derived from a global database, *Glob. Change Biol.*, 13, 2509–2537, doi:10.1111/j.1365-2486.2007.01439.x, 2007.

Mahecha, M. D., Reichstein, M., Carvalhais, N., Lasslop, G., Lange, H., Seneviratne, S. I., Vargas, R., Ammann, C., Arain, M. A. A., Cescatti, A., Janssens, I. A., Migliavacca, M., Montagnani, L., and Richardson, A. D.: Global convergence in the temperature sensitivity of
20 respiration at ecosystem level, *Science*, 329, 838–840, doi:10.1126/science.1189587, 2010.

Malhi, Y., Baldocchi, D. D., and Jarvis, P. G.: The carbon balance of tropical, temperate and boreal forests, *Plant Cell Environ.*, 22, 715–740, doi:10.1046/j.1365-3040.1999.00453.x,
1999.

25 Migliavacca, M., Reichstein, M., Richardson, A. D., Colombo, R., Sutton, M. A., Lasslop, G., Tomelleri, E., Wohlfahrt, G., Carvalhais, N., Cescatti, A., Mahecha, M. D., Montagnani, L., Papale, D., Zaehle, S., Arain, A., Arneth, A., Black, T. A., Carrara, A., Dore, S., Gianelle, D., Helfter, C., Hollinger, D., Kutsch, W. L., Lafleur, P. M., Nouvellon, Y., Rebmann, C., Da Rocha, H. R., Rodeghiero, M., Rouspard, O., Sebastia, M.-T., Seufert, G., Soussana, J.-F., and Van Der Molen, M. K.: Semiempirical modeling of abiotic and biotic factors controlling
30 ecosystem respiration across eddy covariance sites, *Glob. Change Biol.*, 17, 390–409, doi:10.1111/j.1365-2486.2010.02243.x, 2011.

Nishina, K., Ito, A., Beerling, D. J., Cadule, P., Ciais, P., Clark, D. B., Falloon, P., Friend, A. D., Kahana, R., Kato, E., Keribin, R., Lucht, W., Lomas, M., Rademacher, T. T., Pavlick, R.,

**Global
spatiotemporal
distribution of soil
respiration**S. Hashimoto et al.

[Title Page](#)[Abstract](#)[Introduction](#)[Conclusions](#)[References](#)[Tables](#)[Figures](#)[◀](#)[▶](#)[◀](#)[▶](#)[Back](#)[Close](#)[Full Screen / Esc](#)[Printer-friendly Version](#)[Interactive Discussion](#)

Global spatiotemporal distribution of soil respiration

S. Hashimoto et al.

Title Page

Abstract

Introduction

Conclusions

References

Tables

Figures

⏪

⏩

◀

▶

Back

Close

Full Screen / Esc

Printer-friendly Version

Interactive Discussion



Schaphoff, S., Vuichard, N., Warszawski, L., and Yokohata, T.: Quantifying uncertainties in soil carbon responses to changes in global mean temperature and precipitation, *Earth Syst. Dynam.*, 5, 197–209, doi:10.5194/esd-5-197-2014, 2014.

Post, W. M., Emanuel, W. R., Zinke, P. J., and Stangenberger, A. G.: Soil carbon pools and world life zones, *Nature*, 298, 156–159, 1982.

Potter, C. and Klooster, S.: Interannual variability in soil trace gas (CO₂, N₂O, NO) fluxes and analysis of controllers, *Global Biogeochem. Cy.*, 12, 621–635, doi:10.1029/98gb02425, 1997.

Le Quéré, C., Raupach, M. R., Canadell, J. G., Marland, G., Le Quéré, C., Marland, G., Bopp, L., Ciais, P., Conway, T. J., Doney, S. C., Feely, R. A., Foster, P., Friedlingstein, P., Gurney, K., Houghton, R. A., House, J. I., Huntingford, C., Levy, P. E., Lomas, M. R., Majkut, J., Metzler, N., Ometto, J. P., Peters, G. P., Prentice, I. C., Randerson, J. T., Running, S. W., Sarmiento, J. L., Schuster, U., Sitch, S., Takahashi, T., Viovy, N., van der Werf, G. R., and Woodward, F. I.: Trends in the sources and sinks of carbon dioxide, *Nat. Geosci.*, 2, 831–836, doi:10.1038/ngeo689, 2009.

Le Quéré, C., Peters, G. P., Andres, R. J., Andrew, R. M., Boden, T. A., Ciais, P., Friedlingstein, P., Houghton, R. A., Marland, G., Moriarty, R., Sitch, S., Tans, P., Arneeth, A., Arvanitis, A., Bakker, D. C. E., Bopp, L., Canadell, J. G., Chini, L. P., Doney, S. C., Harper, A., Harris, I., House, J. I., Jain, A. K., Jones, S. D., Kato, E., Keeling, R. F., Klein Goldewijk, K., Körtzinger, A., Koven, C., Lefèvre, N., Maignan, F., Omar, A., Ono, T., Park, G.-H., Pfeil, B., Poulter, B., Raupach, M. R., Regnier, P., Rödenbeck, C., Saito, S., Schwinger, J., Segschneider, J., Stocker, B. D., Takahashi, T., Tilbrook, B., van Heuven, S., Viovy, N., Wanninkhof, R., Wiltshire, A., and Zaehle, S.: Global carbon budget 2013, *Earth Syst. Sci. Data*, 6, 235–263, doi:10.5194/essd-6-235-2014, 2014.

R Core team: R: a Language and Environment for Statistical Computing, R Foundation for Statistical Computing, Vienna, 2013.

Raich, J. and Potter, C.: Global patterns of carbon dioxide emissions from soils, *Global Biogeochem. Cy.*, 9, 23–36, 1995.

Raich, J. and Schlesinger, W.: The global carbon dioxide flux in soil respiration and its relationship to vegetation and climate, *Tellus B*, 44, 81–99, 1992.

Raich, J. W., Potter, C. S., and Bhagawati, D.: Interannual variability in global soil respiration, 1980–94, *Glob. Change Biol.*, 8, 800–812, doi:10.1046/j.1365-2486.2002.00511.x, 2002.

Global spatiotemporal distribution of soil respiration

S. Hashimoto et al.

Title Page

Abstract

Introduction

Conclusions

References

Tables

Figures

◀

▶

◀

▶

Back

Close

Full Screen / Esc

Printer-friendly Version

Interactive Discussion



- Reichstein, M., Rey, A., Freibauer, A., Tenhunen, J., Valentini, R., Banza, J., Casals, P., Cheng, Y., Grünzweig, J. M., Irvine, J., Joffre, R., Law, B. E., Loustau, D., Miglietta, F., Oechel, W., Ourcival, J.-M., Pereira, J. S., Peressotti, A., Ponti, F., Qi, Y., Rambal, S., Rayment, M., Romanya, J., Rossi, F., Tedeschi, V., Tirone, G., Xu, M., and Yakir, D.: Modeling temporal and large-scale spatial variability of soil respiration from soil water availability, temperature and vegetation productivity indices, *Global Biogeochem. Cy.*, 17, 1104, doi:10.1029/2003GB002035, 2003.
- Ricciuto, D. M., Davis, K. J., and Keller, K.: A Bayesian calibration of a simple carbon cycle model: the role of observations in estimating and reducing uncertainty, *Global Biogeochem. Cy.*, 22, GB2030, doi:10.1029/2006GB002908, 2008.
- Schlesinger, W. H.: Carbon balance in terrestrial detritus, *Annu. Rev. Ecol. Syst.*, 8, 51–81, 1977.
- Schlesinger, W. H. and Andrews, J.: Soil respiration and the global carbon cycle, *Biogeochemistry*, 48, 7–20, doi:10.1023/A:1006247623877, 2000.
- Smith, P. and Fang, C.: Carbon cycle: a warm response by soils, *Nature*, 464, 499–500, 2010.
- Subke, J.-A., and Bahn, M.: On the “temperature sensitivity” of soil respiration: can we use the immeasurable to predict the unknown?, *Soil Biol. Biochem.*, 42, 1653–1656, doi:10.1016/j.soilbio.2010.05.026, 2010.
- Taylor, K. E., Stouffer, R. J., and Meehl, G. A.: An overview of CMIP5 and the experiment design, *B. Am. Meteorol. Soc.*, 93, 485–498, doi:10.1175/BAMS-D-11-00094.1, 2012.
- Todd-Brown, K. E. O., Randerson, J. T., Post, W. M., Hoffman, F. M., Tarnocai, C., Schuur, E. A. G., and Allison, S. D.: Causes of variation in soil carbon simulations from CMIP5 Earth system models and comparison with observations, *Biogeosciences*, 10, 1717–1736, doi:10.5194/bg-10-1717-2013, 2013.
- Trumbore, S.: Carbon respired by terrestrial ecosystems—recent progress and challenges, *Glob. Change Biol.*, 2, 141–153, doi:10.1111/j.1365-2486.2006.01067.x, 2006.
- Tuomi, M., Vanhala, P., Karhu, K., Fritze, H., and Liski, J.: Heterotrophic soil respiration – comparison of different models describing its temperature dependence, *Ecol. Model.*, 211, 182–190, doi:10.1016/j.ecolmodel.2007.09.003, 2008.
- University of East Anglia Climatic Research Unit (CRU) (Jones, P. and Harris, I.): CRU TS3.21: Climatic Research Unit (CRU) Time-Series (TS) Version 3.21 of High Resolution Gridded Data of Month-by-month Variation in Climate (Jan. 1901–Dec. 2012), doi:10.5285/D0E1585D-3417-485F-87AE-4FCECF10A992, 2013.

- Van Oijen, M., Rougier, J., and Smith, R.: Bayesian calibration of process-based forest models: bridging the gap between models and data, *Tree Physiol.*, 25, 915–927, 2005.
- Wang, X., Piao, S., Ciais, P., Janssens, I. A., Reichstein, M., Peng, S., and Wang, T.: Are ecological gradients in seasonal Q_{10} of soil respiration explained by climate or by vegetation seasonality?, *Soil Biol. Biochem.*, 42, 1728–1734, doi:10.1016/j.soilbio.2010.06.008, 2010.
- Wei, W., Weile, C., and Shaopeng, W.: Forest soil respiration and its heterotrophic and autotrophic components: global patterns and responses to temperature and precipitation, *Soil Biol. Biochem.*, 42, 1236–1244, doi:10.1016/j.soilbio.2010.04.013, 2010.
- Zhou, T., Shi, P., Hui, D., and Luo, Y.: Global pattern of temperature sensitivity of soil heterotrophic respiration (Q_{10}) and its implications for carbon-climate feedback, *J. Geophys. Res.*, 114, G02016, doi:10.1029/2008JG000850, 2009.
- Zobitz, J. M., Moore, D. J. P., Sacks, W. J., Monson, R. K., Bowling, D. R., and Schimel, D. S.: Integration of process-based soil respiration models with whole-ecosystem CO_2 measurements, *Ecosystems*, 11, 250–269, doi:10.1007/s10021-007-9120-1, 2008.

BGD

12, 4331–4364, 2015

**Global
spatiotemporal
distribution of soil
respiration**

S. Hashimoto et al.

Title Page

Abstract

Introduction

Conclusions

References

Tables

Figures

◀

▶

◀

▶

Back

Close

Full Screen / Esc

Printer-friendly Version

Interactive Discussion



Global spatiotemporal distribution of soil respiration

S. Hashimoto et al.

Table 1. A priori and a posteriori probability distributions of the parameters. The MAP is the maximum a posteriori estimate. A uniform distribution was assumed for every a priori distribution. CI indicates the confidence interval. F , a , b , K , and α are the model parameters, and σ is the standard deviation of the model-data error.

Parameters	Prior	MAP	Mean	Median	SD	95% CI	Kurtosis	Geweke's P	Geweke's Z
F	0.1–5.0	1.68	1.76	1.76	0.15	1.478–2.049	2.83	0.59	0.22
a	0.001–0.1	0.0528	0.049	0.049	0.01	0.0335–0.0725	2.99	0.32	–0.48
b	0.00001–0.005	0.000628	0.0006	0.0005	0.0003	0.0001–0.0012	2.97	0.31	–0.50
K	0.01–10.0	1.20	1.46	1.42	0.35	0.861–2.211	3.00	0.45	–0.12
α	0.0–1.0	0.98	0.47	0.41	0.33	0.0254–0.987	1.56	0.51	0.03
σ	100.0–1500.0	375.5	377.6	377.5	6.61	365.0–390.8	3.07	0.52	0.05

Title Page

Abstract

Introduction

Conclusions

References

Tables

Figures



Back

Close

Full Screen / Esc

Printer-friendly Version

Interactive Discussion



Global spatiotemporal distribution of soil respiration

S. Hashimoto et al.

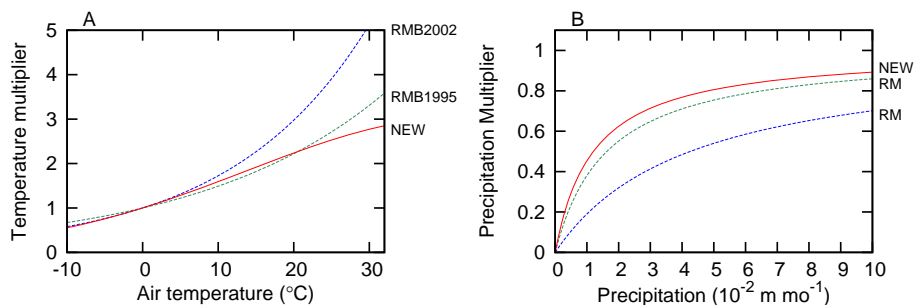


Figure 1. Shapes of the temperature function (a) and precipitation function (b). The red line represents the results of this study, and the green-dashed and blue-dashed lines indicate the functions estimated by previous studies (Raich and Potter, 1995; Raich et al., 2002).

[Title Page](#)[Abstract](#)[Introduction](#)[Conclusions](#)[References](#)[Tables](#)[Figures](#)[◀](#)[▶](#)[◀](#)[▶](#)[Back](#)[Close](#)[Full Screen / Esc](#)[Printer-friendly Version](#)[Interactive Discussion](#)

Global spatiotemporal distribution of soil respiration

S. Hashimoto et al.

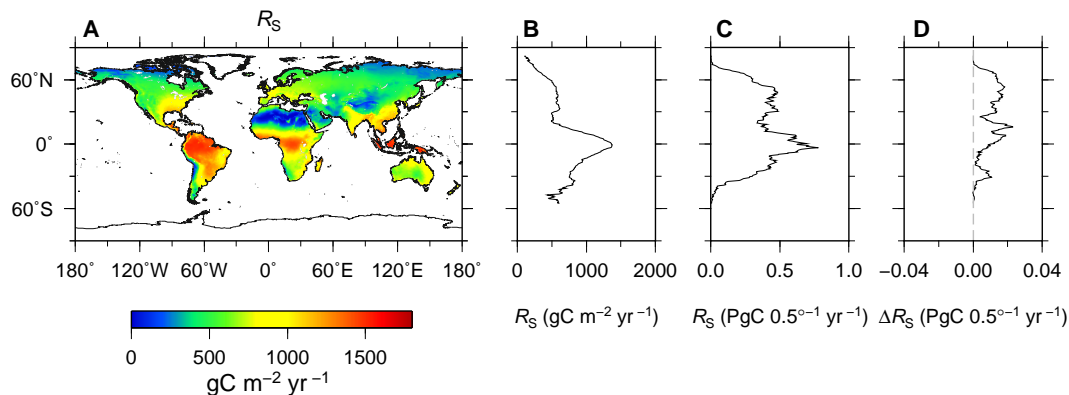


Figure 2. Spatial distribution of the estimated annual soil respiration (a), the latitudinal patterns of soil respiration components (b and c), and difference between the earlier (1965–1989) and later (1990–2012) periods of the simulation (d).

[Title Page](#)[Abstract](#)[Introduction](#)[Conclusions](#)[References](#)[Tables](#)[Figures](#)[◀](#)[▶](#)[◀](#)[▶](#)[Back](#)[Close](#)[Full Screen / Esc](#)[Printer-friendly Version](#)[Interactive Discussion](#)

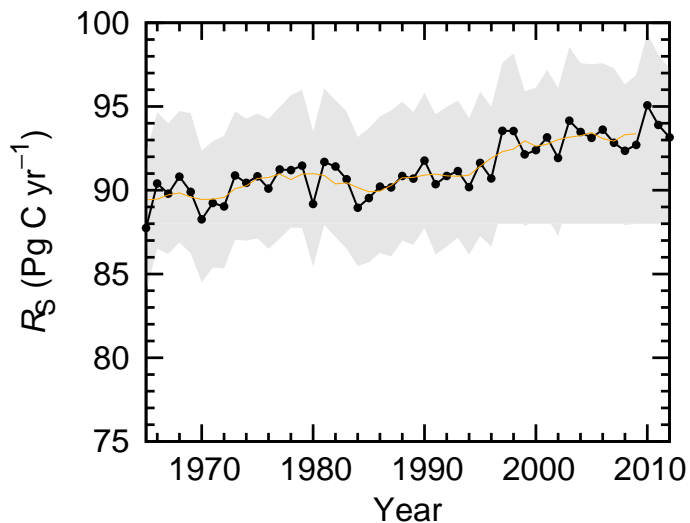


Figure 3. Temporal variation of the estimated global soil respiration. The grey region indicates the 95 % confidence limits of the Monte Carlo simulation ($N = 1000$). The orange line represents the 5 year moving average.

Global spatiotemporal distribution of soil respiration

S. Hashimoto et al.

[Title Page](#)

[Abstract](#) | [Introduction](#)

[Conclusions](#) | [References](#)

[Tables](#) | [Figures](#)

[◀](#) | [▶](#)

[◀](#) | [▶](#)

[Back](#) | [Close](#)

[Full Screen / Esc](#)

[Printer-friendly Version](#)

[Interactive Discussion](#)



Global spatiotemporal distribution of soil respiration

S. Hashimoto et al.

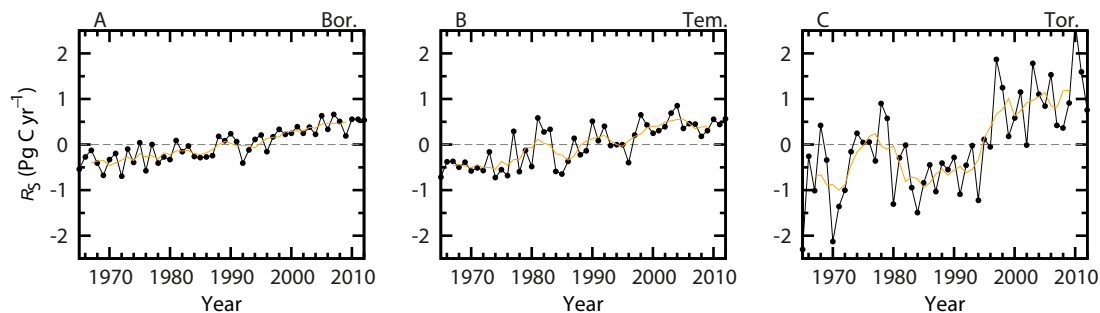


Figure 4. Interannual variations of soil respiration for boreal, temperate, and tropical regions. The orange lines represent the 5 year moving averages.

[Title Page](#)[Abstract](#)[Introduction](#)[Conclusions](#)[References](#)[Tables](#)[Figures](#)[Back](#)[Close](#)[Full Screen / Esc](#)[Printer-friendly Version](#)[Interactive Discussion](#)

Global
spatiotemporal
distribution of soil
respiration

S. Hashimoto et al.

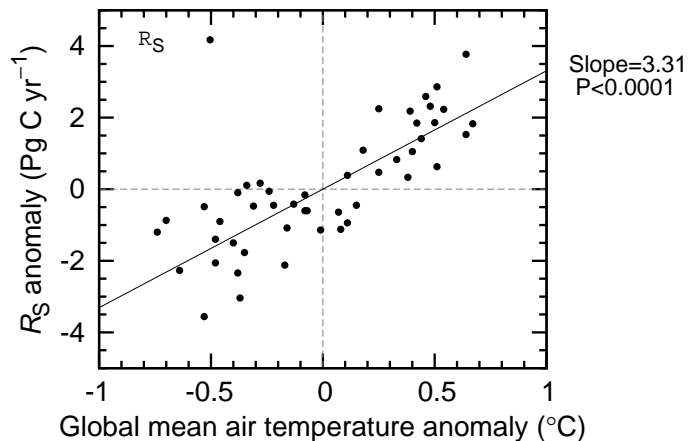


Figure 5. Relationship between the global mean air-temperature anomaly and the soil-respiration anomaly. The anomaly was calculated as the deviation from the 1965–2012 mean.

[Title Page](#)[Abstract](#)[Introduction](#)[Conclusions](#)[References](#)[Tables](#)[Figures](#)[◀](#)[▶](#)[◀](#)[▶](#)[Back](#)[Close](#)[Full Screen / Esc](#)[Printer-friendly Version](#)[Interactive Discussion](#)

BGD

12, 4331–4364, 2015

Global spatiotemporal distribution of soil respiration

S. Hashimoto et al.

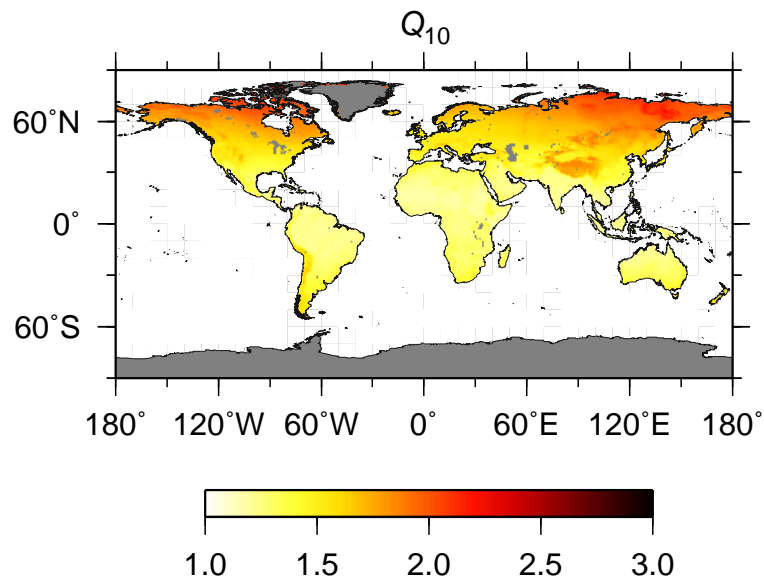


Figure 6. Spatial distribution of Q_{10} values estimated using the temperature function and the mean temperature of each grid.

[Title Page](#)[Abstract](#)[Introduction](#)[Conclusions](#)[References](#)[Tables](#)[Figures](#)[◀](#)[▶](#)[◀](#)[▶](#)[Back](#)[Close](#)[Full Screen / Esc](#)[Printer-friendly Version](#)[Interactive Discussion](#)

Global spatiotemporal distribution of soil respiration

S. Hashimoto et al.

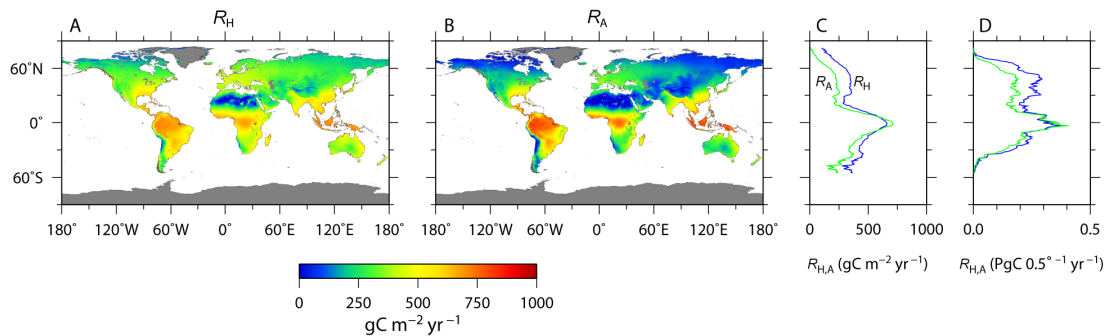


Figure 7. Spatial distribution of heterotrophic respiration (a) and autotrophic respiration (b). (c and d) depict the latitudinal distributions of heterotrophic and autotrophic respiration per square meter and per 0.5° , respectively.

[Title Page](#)[Abstract](#)[Introduction](#)[Conclusions](#)[References](#)[Tables](#)[Figures](#)[◀](#)[▶](#)[◀](#)[▶](#)[Back](#)[Close](#)[Full Screen / Esc](#)[Printer-friendly Version](#)[Interactive Discussion](#)

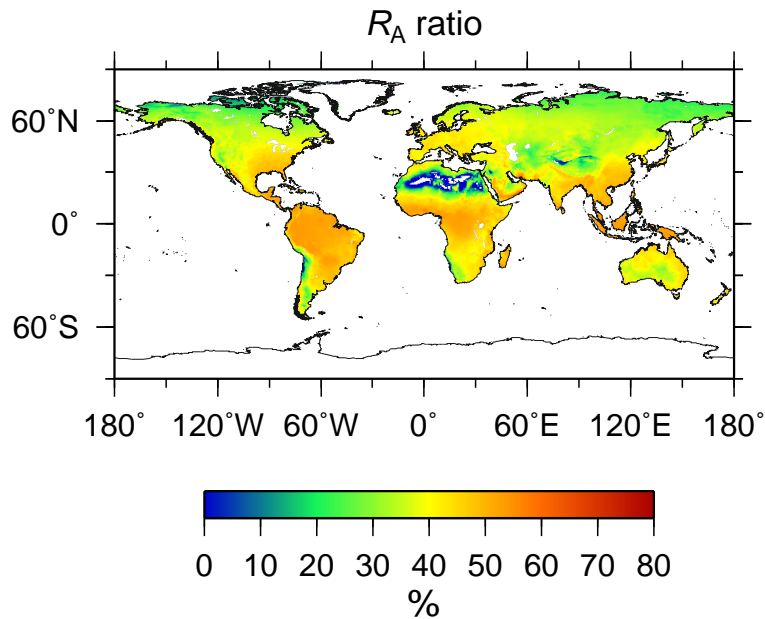


Figure 8. Distribution of the ratio of autotrophic respiration to total soil respiration.

**Global
spatiotemporal
distribution of soil
respiration**

S. Hashimoto et al.

[Title Page](#)

Abstract	Introduction
Conclusions	References
Tables	Figures

⏪	⏩
◀	▶

Back	Close
----------------------	-----------------------

[Full Screen / Esc](#)

[Printer-friendly Version](#)

[Interactive Discussion](#)



Global spatiotemporal distribution of soil respiration

S. Hashimoto et al.

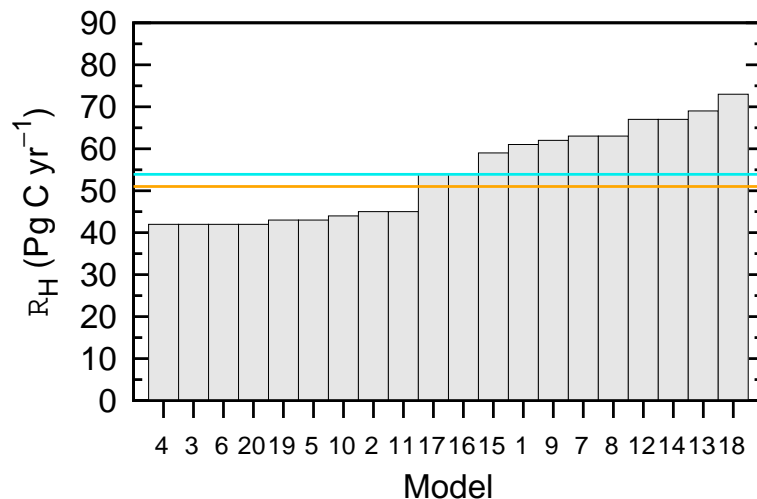


Figure 9. Comparison of global heterotrophic respiration. The grey bars are the results from the 20 Earth system models of the CMIP5 (1965–2004; please see Table S3). The orange line represents the result of this study. The blue line indicates the mean of the results of the 20 Earth system models.

Title Page

Abstract

Introduction

Conclusions

References

Tables

Figures

◀

▶

◀

▶

Back

Close

Full Screen / Esc

Printer-friendly Version

Interactive Discussion



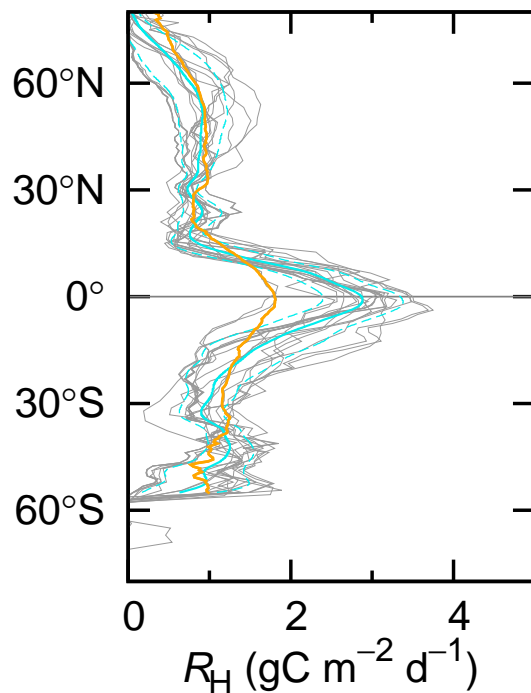


Figure 10. Latitudinal distribution of heterotrophic respiration. The orange line represents the results of this study. The grey lines are the results from the 20 Earth system models (please see Table S3). A smoothing spline was fit to each result because of the variation in the grid sizes of the Earth system models. The solid blue lines and broken blue lines indicate the mean and standard deviation, respectively, of the results of the 20 Earth system models.